International Journal of Nanomedicine

Dovepress
open access to scientific and medical research

Open Access Full Text Article

ORIGINAL RESEARCH

Atomic layer deposition of nano-TiO_2 thin films with enhanced biocompatibility and antimicrobial activity for orthopedic implants

This article was published in the following Dove Press journal:
International Journal of Nanomedicine

Luting Liu[1]
Ritwik Bhatia[2]
Thomas J Webster[1,3]

[1]Department of Chemical Engineering, Northeastern University, Boston, [2]Ultratech Inc., Waltham, MA, USA; [3]Wenzhou Institute of Biomaterials and Engineering, Wenzhou Medical University, Wenzhou, People's Republic of China

Abstract: Titanium (Ti) and its alloys have been extensively used as implant materials in orthopedic applications. Nevertheless, implants may fail due to a lack of osseointegration and/or infection. The aim of this in vitro study was to endow an implant surface with favorable biological properties by the dual modification of surface chemistry and nanostructured topography. The application of a nanostructured titanium dioxide (TiO_2) coating on Ti-based implants has been proposed as a potential way to enhance tissue-implant interactions while inhibiting bacterial colonization simultaneously due to its chemical stability, biocompatibility, and antimicrobial properties. In this paper, temperature-controlled atomic layer deposition (ALD) was introduced for the first time to provide unique nanostructured TiO_2 coatings on Ti substrates. The effect of nano-TiO_2 coatings with different morphology and structure on human osteoblast and fibroblast functions and bacterial activities was investigated. In vitro results indicated that the TiO_2 coating stimulated osteoblast adhesion and proliferation while suppressing fibroblast adhesion and proliferation compared to uncoated materials. In addition, the introduction of nano-TiO_2 coatings was shown to inhibit gram-positive bacteria (*Staphylococcus aureus*), gram-negative bacteria (*Escherichia coli*), and antibiotic-resistant bacteria (methicillin-resistant *Staphylococcus aureus*), all without resorting to the use of antibiotics. Our results suggest that the increase in nanoscale roughness and greater surface hydrophilicity (surface energy) together could contribute to increased protein adsorption selectively, which may affect the cellular and bacterial activities. It was found that ALD-grown TiO_2-coated samples with a moderate surface energy at 38.79 mJ/m^2 showed relatively promising antibacterial properties and desirable cellular functions. The ALD technique provides a novel and effective strategy to produce TiO_2 coatings with delicate control of surface nanotopography and surface energy to enhance the interfacial biocompatibility and mitigate bacterial infection, and could potentially be used for improving numerous orthopedic implants.

Keywords: atomic layer deposition, titanium dioxide, nanostructure, osteoblast, fibroblast, antimicrobial activity

Introduction

Orthopedic implants are widely used devices implanted into the human body, with the aim of permanently supporting fractured or replacing disease-damaged bones for pain relief and functional improvement. Titanium (Ti)-based materials, as a representative of metallic biomaterials, are recognized as the most promising materials for orthopedic implants.[1] Ti itself is considered a bioinert material with good biocompatibility, excellent corrosion resistance, and appropriate mechanical properties. It is well known that a stable titanium dioxide (TiO_2) layer of 3–10 nm in thickness spontaneously forms

Correspondence: Thomas J Webster
Department of Chemical Engineering, 313 Snell Engineering Center, Northeastern University, 360 Huntington Ave., Boston, MA 02115, USA
Tel +1 617 373 6585
Email th.webster@neu.edu

submit your manuscript | www.dovepress.com
Dovepress
http://dx.doi.org/10.2147/IJN.S148065

when Ti is exposed to air or water, endowing the surface with biocompatibility.[2] Nevertheless, implants may still fail due to a lack of integration with bone tissue and/or infection.[3–5] For example, it has been reported that ~10% of these implants fail prematurely within the first 10–20 years, and 18% of implant failures have been due to aseptic loosening, while 20% of failures have been attributed to infection.[6] In recent years, most research so far has focused on the design of implant surfaces either to prevent infection while ignoring osseointegration or vice versa. For example, silver nanoparticle technology is receiving much interest in the field of orthopedics for its antimicrobial properties; however, at present, concerns have been raised regarding their toxic effect on mammalian cells.[7,8] For a successful implant, strong osseointegration and anti-infection properties are indispensable, necessitating implant designs to satisfy both simultaneously.[9]

It is clear that both chemical and physical properties of the surface play a major role in modulating the biological events directly at the tissue-implant interface.[10–12] For Ti-based implants, the naturally formed TiO_2 thin layers are thought to act as a barrier between the implant and tissue to prevent metallic ion release into the body and consequently minimizing the chances of an immune response; however, recent studies have indicated that this few-nanometer-thin layer does not provide sufficient long-term corrosion protection.[2,13] Understanding the role of this native TiO_2 film on biomedical Ti implants paves the way for in-depth studies focused on developing a multifunctional Ti implant surface by modifying and structuring the natural oxide layer to further improve biocompatibility. On the other hand, TiO_2 in the form of coatings has also been extensively exploited for antibacterial activities due to photocatalysis, demonstrating a promising potential in fighting against infections without sacrificing osseointegration.[14–16] Additionally, it has been reported that the physical topography and structure of the implant surfaces can be optimized down to the nanoscale to produce favorable surface properties (ie, surface roughness, surface wettability, surface energy, surface phase, etc.) to promote desirable cell functions while minimizing bacterial colonization.[17–20] Taking all these into consideration, functionalizing Ti implant surfaces via deposition of a thin, nano-TiO_2 coating presents an attractive way to tailor the bioactivity of implant material, and hence the osseointegration and disinfection of the implant.

Various techniques have been employed to prepare TiO_2 coatings, including e-beam evaporation, sputtering, sol-gel spinning, pulsed laser deposition, chemical vapor deposition, and atomic layer deposition (ALD).[21–26] In selecting an appropriate deposition technology for this specific application, several criteria have to be considered such as coating morphology, deposition rate and coverage, interfacial quality, and industrial applicability. Among these methods, the ALD process is based on the sequential use of self-terminating surface reactions, which is perfect for the deposition of metal oxide layers with atomic layer control on geometrical nanostructures with high aspect ratios. Compared with other more common techniques, ALD possesses several advantages in the deposition of TiO_2, such as precise thickness control, extremely conformal coating for nanostructures, excellent large-area uniformity, strong bonding strength, low growth temperature, good reproducibility and straightforward scale-up, and applicability to sensitive substrates (ie, biomaterials).[25]

For deposition of TiO_2 by the ALD processes, various metal-organic precursors exist; some of the most commonly used precursors are titanium tetrachloride, titanium isopropoxide, and tetrakis(dimethylamino)titanium (TDMATi) in combination with water (H_2O) or ozone as an oxidant.[27,28] Since the bond energy of metal-halide is much stronger than that of the metal-nitrogen bond, metal amide compounds are expected to have much higher reactivity with H_2O and, therefore, TDMATi and H_2O have been used for ALD processes. In addition, they possess the advantage that precursors and decomposition products are non-toxic and non-corrosive.[29] A growth regime with a linear increase in layer thickness with the number of ALD cycles has been reported for deposition temperatures ranging from 50°C to 300°C.[30] Numerous studies have reported the formation of homogeneous amorphous films at relatively low temperatures and rough anatase surfaces at high temperatures.[31–33] Therefore, in this study, nano-TiO_2 thin films were deposited on commercial Ti substrates by ALD using TDMATi and H_2O. The effect of surface morphology and structure of the TiO_2 layer at different temperatures were investigated here. The antibacterial properties of the as-grown TiO_2 thin films against three different types of bacteria (*Staphylococcus aureus*, *Escherichia coli*, and methicillin-resistant *Staphylococcus aureus* [MRSA]) were determined and the cellular biological effects with osteoblasts and fibroblasts were studied in vitro. Furthermore, the role of surface wettability/surface energy to changes in specific protein adsorption and biological activities (ie, cell adhesion and bacterial growth) was correlated.

Materials and methods

ALD-grown TiO_2 sample preparation

From Alfa Aesar, 99.5% Ti foils (0.25 mm thick, annealed) were purchased. All the chemicals related to the ALD process

were provided by Ultratech, Inc. (Waltham, MA, USA); others were purchased from Sigma-Aldrich. Ti samples were cut into identical size pieces (1×1 cm^2) and were cleaned with acetone, 70% ethanol, and deionized water (Milli-Q water) separately, each for 15 minutes. Then, the cleaned samples were placed in an ALD chamber. The TiO_2 thin films were deposited onto the Ti substrates using TDMATi and H_2O as ALD precursors, and N_2 served as a purging gas. In this study, a standard ALD cycle consisted of a 0.1 second exposure to TDMATi, a 6 second N_2 purge, a 0.1 second exposure to H_2O, and a 6 second N_2 purge. The total flow rate of the N_2 was 100 sccm. The TiO_2 thin films were grown at a temperature of 120°C, 160°C, and 190°C. A total of 2,500 cycles corresponding to ~100 nm of the TiO_2 film were carried out.

All the samples were sterilized by ultrasonication in 70% ethanol followed by UV irradiation (30 minutes) for the biological experiments.

Surface characterization

Surface morphology, composition, phase, and roughness measurements

All the samples were thoroughly rinsed with deionized water and then dried at room temperature. The surface morphology of the samples was characterized by scanning electron microscopy (SEM; Hitachi S-4800). Compositional analysis was conducted using EDAX. For surface roughness measurements, an atomic force microscope (AFM; Parks Scientific XE-7 AFM) was used to scan Ti samples. Each sample was analyzed in ambient air under non-contact mode using a silicone ultrasharp cantilever (probe tip radius of 10 µm; MikroMasch); 1.5×1.5 µm AFM fields were analyzed and the scan rate was chosen as 0.4 Hz. Image analysis software (XEI) was used to generate micrographs and to quantitatively compare the root-mean-square (RMS) roughness of the samples. The crystallinity of the films was investigated using an X-ray diffractometer (XRD; Ultima, Rigaku Corp.) fitted with a Cu Kα radiation. The XRD was operated at 40 kV and 44 mA with a step size of 0.02° and a scanning range of 2θ=20°–60°. Phase identification was performed using the standard JCPDS database. Experiments were completed in triplicate.

Surface wettability and surface energy measurements

The surface wettability and surface energy of the substrates of interest were measured by contact angles. Contact angle measurements were conducted and analyzed automatically using a SEO Phoenix 300 Contact Angle Measurement System. One droplet each (5 µL) of deionized water, ethanol, and ethylene glycol was added on top of the substrates of interest by controlling injection. The contact angle was immediately measured 5 seconds after placing the drop on each sample and the test was conducted at room temperature. Measurements were performed three times, the average contact angle was determined, and results were used to calculate the surface free energy according to the Owens–Wendt method.[34]

$$(1+\cos\theta)\,\gamma_1 = 2\left(\sqrt{\gamma_1^d \gamma_s^d} + \sqrt{\gamma_1^p \gamma_s^p}\right)$$

Here, γ_s^d and γ_s^p are the dispersive and polar components of the substrate surface energy, γ_s; γ_1^d and γ_1^p are the dispersive and polar components of the liquid surface tension, γ_1, respectively; and θ is the contact angle as determined.

Antimicrobial assays

Bacterial inhibitory assays

Bacteria cell lines of *S. aureus* (ATCC 25923), *E. coli* (ATCC 25922), and MRSA (ATCC 43300) were used in this study. All sterilized Ti samples were transferred into 24-well non-tissue culture plates and rinsed twice with phosphate-buffered saline (PBS). Then, the samples were treated with the prepared bacterial solutions at a concentration of 10^6 bacteria/mL in tryptic soy broth (TSB, 0.03 g/mL) and cultured for 24 hours in an incubator (37°C, humidified, 5% CO_2). Afterward, the samples were washed twice with PBS to remove the floating bacteria and were transferred into 15 mL tubes with 3 mL of PBS each. Following this, the samples were sonicated for 10 minutes to release the bacteria attached on the sample surface into the PBS solution. Then, a series of diluted solutions with bacteria were pipetted onto TSB agar plates (3×10 µL spots per dilution) and bacteria colonies were counted after 14 hours of incubation.

Live/dead fluorescent microscopy assays

Samples were prepared and seeded with bacterial solutions as already described. After 2 hours and 24 hours of incubation, the samples were washed three times with PBS and then stained for fluorescence microscopy analysis. The Live/Dead Baclight bacterial viability kit (Life Technologies) was used to view adherent bacteria. Equal volumes of 3.34 mM SYTO 9 dye and 20 mM propidium iodide were mixed together and then added to a 0.85% sodium chloride (NaCl) solution at 3 µL per 1 mL of NaCl. Then, 1 mL of this mixed solution was added onto each sample and allowed to incubate in the dark for 15 minutes. Following this, the samples were turned upside down into a new 24-well plate and viewed using a Zeiss Axio Observer Z1 with Zen 2 Pro Software.

Protein adsorption assays

A bicinchoninic acid (BCA) protein assay kit (Thermo Scientific) was used to quantify the adsorption of the total amount of protein and target protein (casein) in bacterial culture medium to sample surfaces. Each sample was treated separately with 1 mL of sterile TSB and then cultured for 24 hours in an incubator (37°C, humidified, 5% CO_2). After that, samples were transferred to a new 24-well plate and washed twice with PBS to remove non-absorbed proteins. Then, each sample was treated with 0.5 mL RIPA buffer (Sigma-Aldrich) for 10 minutes to solubilize the adsorbed protein. Afterward, the amount of total proteins in the supernatant was tested according to the BCA assay protocol. Casein protein has been shown to be a key protein in TSB medium (17 g casein/L); thus, to quantify casein protein adsorption, we incubated samples with the prepared 1.7% by weight casein solution (17 g casein/L H_2O, Sigma-Aldrich), and then the same procedures, as already described, to determine total protein adsorption were used.

Cell assays

Cell culture

Human osteoblasts (PromoCell, C-12720) and human dermal fibroblasts (Lonza, CC-2509) at population numbers less than 10 were used for all cell experiments. Osteoblasts were cultured in phenol red-free osteoblast basal medium with an osteoblast growth medium supplemental mix (PromoCell) and 1% penicillin/streptomycin (P/S; Sigma-Aldrich). Fibroblasts were cultured in Dulbecco's modified Eagle's medium (ATCC) supplemented with 10% fetal bovine serum (Sigma-Aldrich) and 1% P/S. All cells were cultured at 37°C in a humidified, 5% CO_2/95% air environment.

Cell adhesion and proliferation assays

All the sterilized Ti samples were placed individually into the wells of 24-well tissue culture plates. Before cell seeding, samples were rinsed twice with PBS to remove any possible debris. Cells were then seeded onto the samples at a density of 10,000 cells/cm^2 and were allowed to adhere for 4 hours at 37°C in a humidified 5% CO_2 atmosphere to determine cell adhesion. Cell proliferation was measured after 1, 3, and 5 days of culture. The medium was changed every other day during proliferation trials. After the prescribed incubation time, the samples were washed twice with PBS and were carefully transferred to fresh 24-well tissue culture plates. Then, fresh medium was added to each well along with an MTS dye (Promega) at a 5:1 ratio (medium:MTS). Next, the plates were cultured for another 4 hours to allow the MTS dye to completely react with the metabolic products of the adherent cells, and then 200 µL of the solution from each well was transferred to a 96-well plate in triplicate. Finally, the absorbance was measured at 490 nm by a plate reader (Molecular Devices, SpectraMax M3) to determine cell density.

Statistical analysis

All cell and bacteria studies were conducted in triplicate and repeated at least three times. Data were collected and the significant differences were assessed using ANOVA followed by one-tailed Student's *t*-tests. Statistical significance was considered at $p<0.05$.

Results

Surface morphology, composition, roughness, phase

It has been reported that the choice of the ALD growth temperature enables one to grow TiO_2 films with either very smooth or rough surfaces. Moreover, films with certain crystal structure can be achieved in appropriate growth conditions.[30] The surface morphology of Ti-TiO_2 (ALD treated at 120°C, 160°C, and 190°C) and untreated Ti as a control was visualized by SEM as shown in Figure 1A–D. It was found that the ALD-grown TiO_2 films showed a remarkable increase in surface roughness and noticeable agglomeration occurred with an increase in temperature. Formation of crystallites on the film surfaces can be clearly observed. EDAX spectra (Figure 1E) showed the presence of a remarkable TiO_2 nanoscale coating. The elemental concentration of each sample determined by EDAX as shown in Table 1 indicated that all the TiO_2-coated samples had similar chemical composition, which could be attributed to the precise film thickness control of the ALD process.

AFM measurements were performed to characterize the nanotopography and measure surface roughness of the samples. The RMS roughness obtained by AFM showed increased surface roughness from 12.7 nm (Ti control) to around 40 nm (Ti-TiO_2) (Figure 2). XRD patterns of the samples are shown in Figure 3. All diffraction peaks are in good agreement with the standard JCPDS data. XRD patterns exhibited strong diffraction peaks at 2θ=25.4° and 48.0° for Ti-TiO_2 (190°C) indicating the formation of crystalline anatase TiO_2 films compared with all other samples.

Surface wettability and surface energy

Surface chemistry together with surface topography can affect surface wetting properties (hydrophilicity/

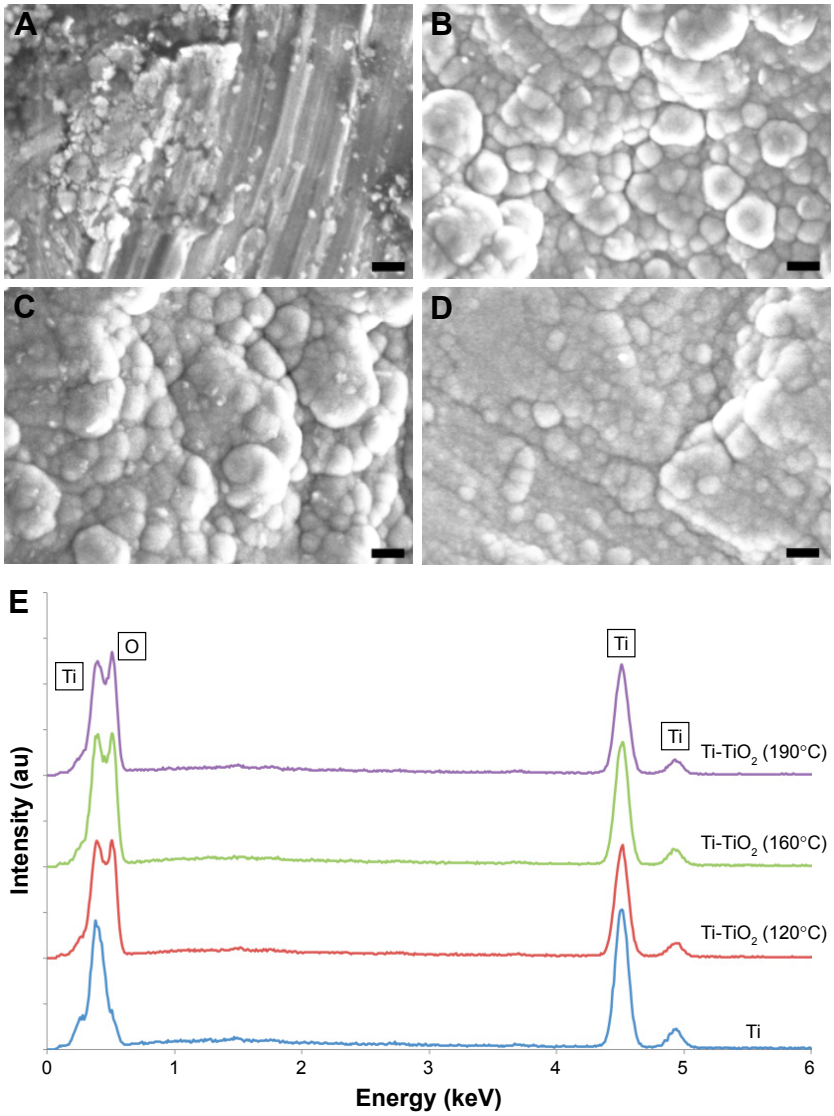

Figure 1 SEM images of (**A**) Ti control, (**B**) Ti-TiO_2 (190°C), (**C**) Ti-TiO_2 (160°C), and (**D**) Ti-TiO_2 (120°C) and (**E**) EDAX spectra of Ti samples. Scale bars are 200 nm.
Abbreviations: O, oxygen; SEM, scanning electron microscopy; Ti, titanium; TiO_2, titanium dioxide.

hydrophobicity) and surface energy, and can also further affect the absorption of proteins to the implant surface, which act as the key factor in mediating cell and bacteria activities at the tissue-implant interface.[35–38] Therefore, contact angle measurements were carried out to determine the surface wettability and surface energy of the Ti-TiO_2 and Ti control samples. By combining the contact angle results from three different liquids, surface energy was obtained based on the Owens–Wendt method. γ_s is the total surface energy, which is composed of polar and dispersive components. The dispersive component theoretically accounts for van der Waals and other non-site specified interactions, and the polar component is associated with dipole-dipole, dipole-induced dipole, hydrogen bonding, and other site-specified interactions. As a whole, the data taken from these experiments indicated that all the ALD-TiO_2-coated surfaces were slightly hydrophilic, and the total surface energy was relatively higher compared to the Ti control surface, as shown in Table 2.

Table 1 The elemental concentration (atomic percentage) in the outermost layer of Ti samples with or without TiO_2 coatings determined by EDAX

Substrates	Ti	O
Ti control	100	0
Ti-TiO_2 (190°C)	48.16±0.10	51.84±0.10
Ti-TiO_2 (160°C)	48.86±0.36	51.14±0.36
Ti-TiO_2 (120°C)	49.48±0.16	50.52±0.16

Note: All experimental samples were statistically ($p<0.01$) different from controls but not different from each other.
Abbreviations: O, oxygen; Ti, titanium; TiO_2, titanium dioxide.

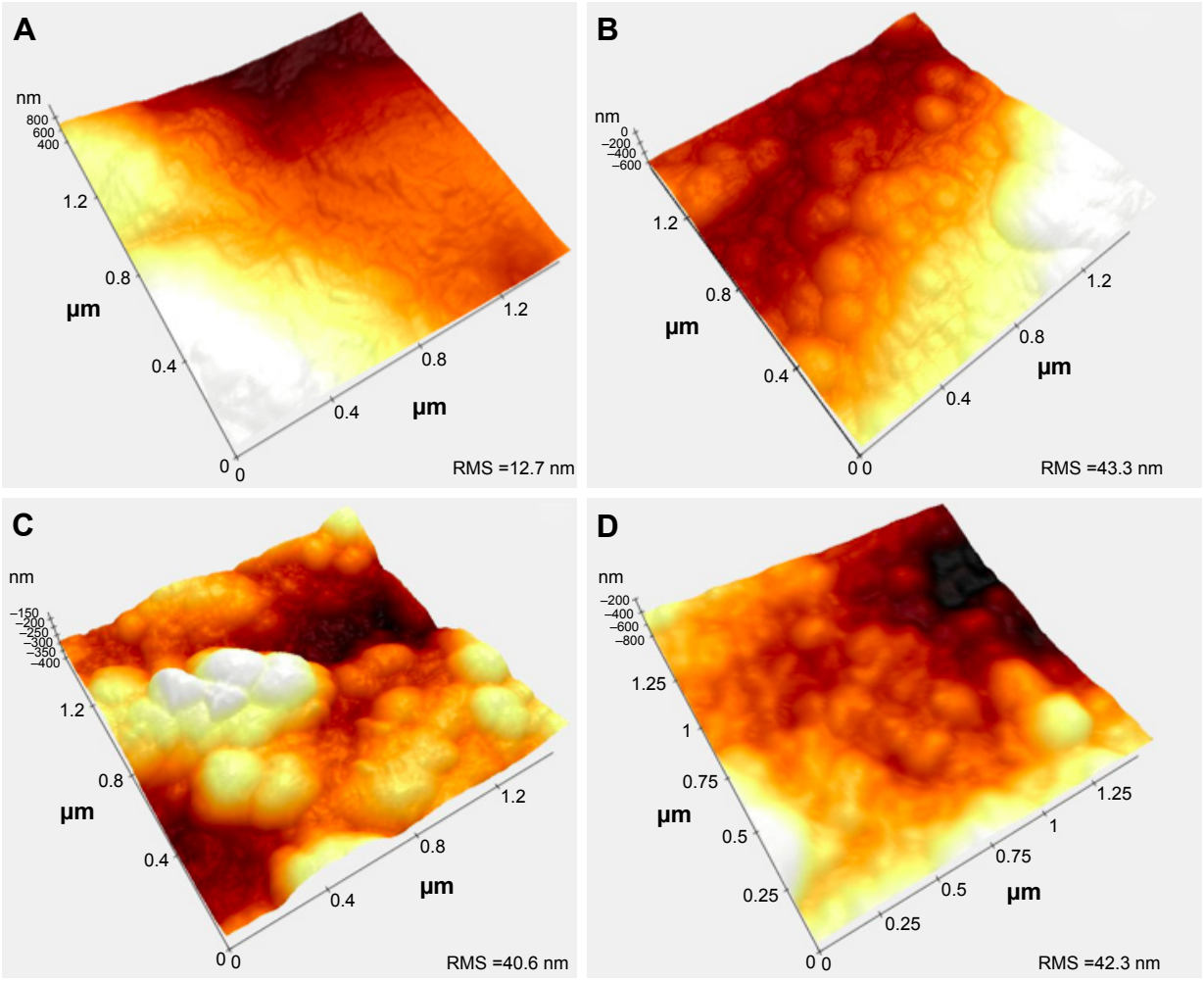

Figure 2 AFM images and RMS roughness values (in nm) of (**A**) Ti control, (**B**) Ti-TiO_2 (190°C), (**C**) Ti-TiO_2 (160°C), and (**D**) Ti-TiO_2 (120°C).
Abbreviations: RMS, root-mean-square; Ti, titanium; TiO_2, titanium dioxide; AFM, atomic force microscopy.

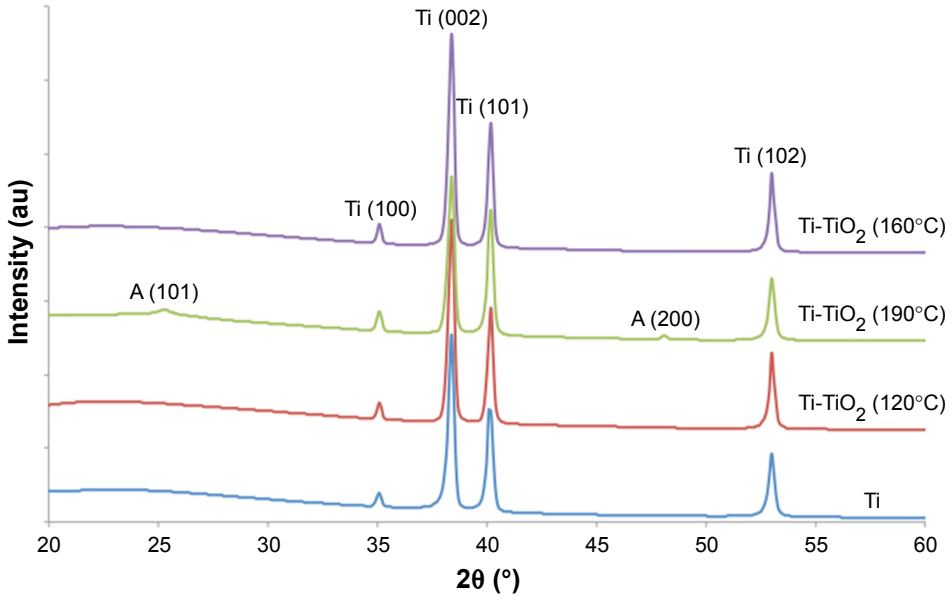

Figure 3 XRD patterns of the Ti samples with different TiO_2 coatings.
Abbreviations: A, anatase; Ti, titanium; TiO_2, titanium dioxide; XRD, X-ray diffraction.

Table 2 Summary of surface wettability and surface energy of Ti samples with different TiO_2 coatings

Substrates	Surface wettability (water contact angle/°)	Surface energy (mJ/m²)		
		γ_s	γ_s^p	γ_s^d
Ti control	70.27±1.16	32.78	9.83	22.95
Ti-TiO_2 (190°C)	55.61±2.43	46.20	6.68	39.52
Ti-TiO_2 (160°C)	62.80±2.00	38.79	13.93	24.87
Ti-TiO_2 (120°C)	53.10±2.76	48.51	6.69	41.82

Notes: Data represent mean ± SD, N=3. All experimental samples had statistically ($p<0.01$) greater total surface energy than controls.
Abbreviations: Ti, titanium; TiO_2, titanium dioxide.

Antimicrobial assays

The effect of these coatings on the activities of three different types of bacteria (gram-positive bacteria, gram-negative bacteria, and antibiotic-resistant bacteria) was determined. In vitro bacterial results indicated that the Ti-TiO_2 samples, specifically Ti-TiO_2 (160°C), inhibited the adhesion and growth of all three different types of bacteria (*S. aureus*, *E. coli*, and MRSA) significantly (exceeding 80%) compared to the results obtained from the Ti control as shown in Figure 4A–C; again, this was accomplished without using antibiotics.

To further analyze these findings, additional fluorescent microscopy experiments employing SYTO® 9/propidium iodide (to distinguish between live and dead bacteria) were carried out. Fluorescent micrographs of *S. aureus* (Figure 5), *E. coli* (Figure 6), and MRSA (Figure 7) cultured for 2 hours and 24 hours on Ti-TiO_2 (160°C) and Ti control samples showed that these TiO_2 coatings not only inhibited bacterial adhesion and growth but also killed the bacteria to some extent.

Protein adsorption assays

Based on the results from protein adsorption assays as shown in Figure 8, the TiO_2-coated samples significantly increased protein adsorption over Ti control samples after being treated with 3% TSB and 1.7% casein protein solution for 24 hours. The increased protein adsorption might play an important role in inhibiting bacteria adhesion and growth, because those

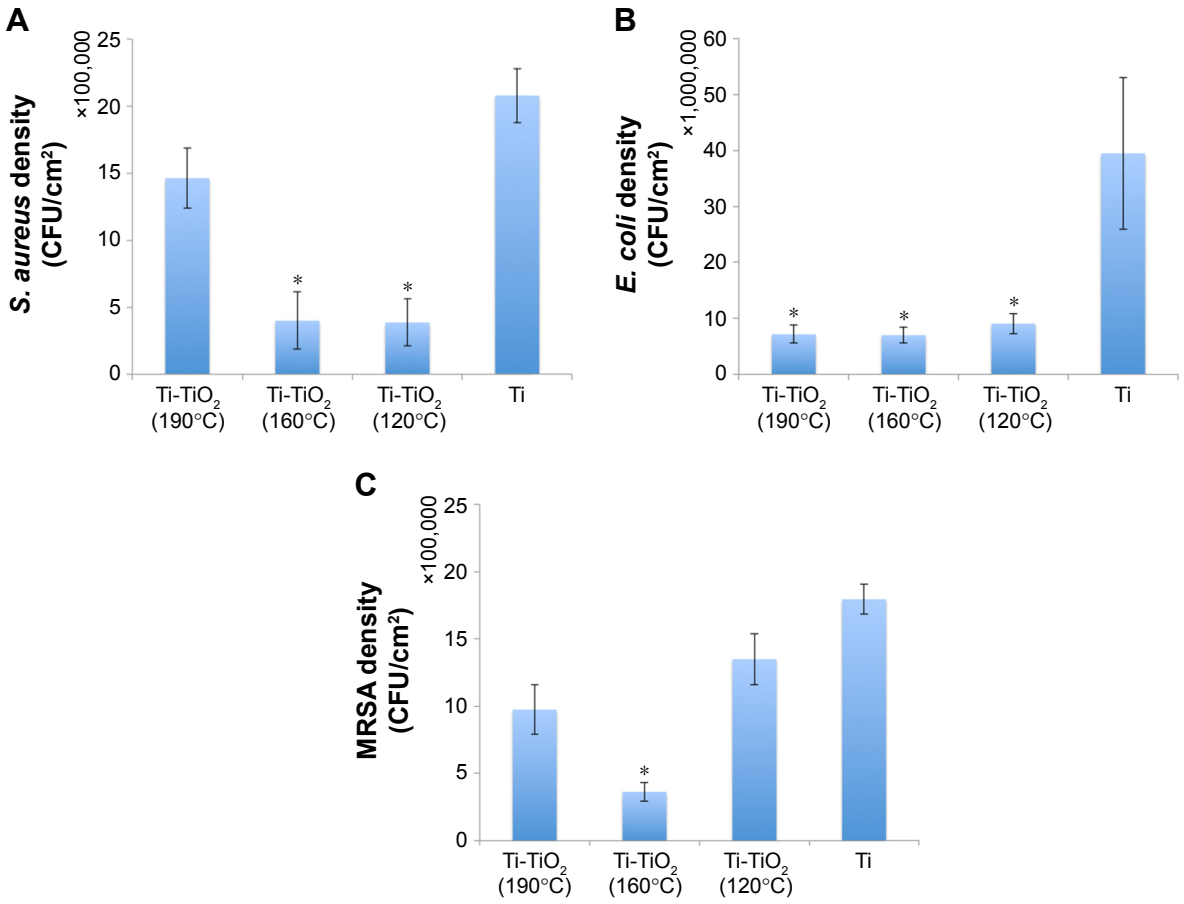

Figure 4 (**A**) *S. aureus*, (**B**) *E. coli*, and (**C**) MRSA growth on Ti samples with different TiO_2 coatings after 24 hours of culture. Data represent mean ± SD, N=3. *$p<0.05$ compared with Ti control (labeled as Ti).
Abbreviations: *S. aureus*, *Staphylococcus aureus*; *E. coli*, *Escherichia coli*; MRSA, methicillin-resistant *Staphylococcus aureus*; Ti, titanium; TiO_2, titanium dioxide; CFU, colony-forming unit.

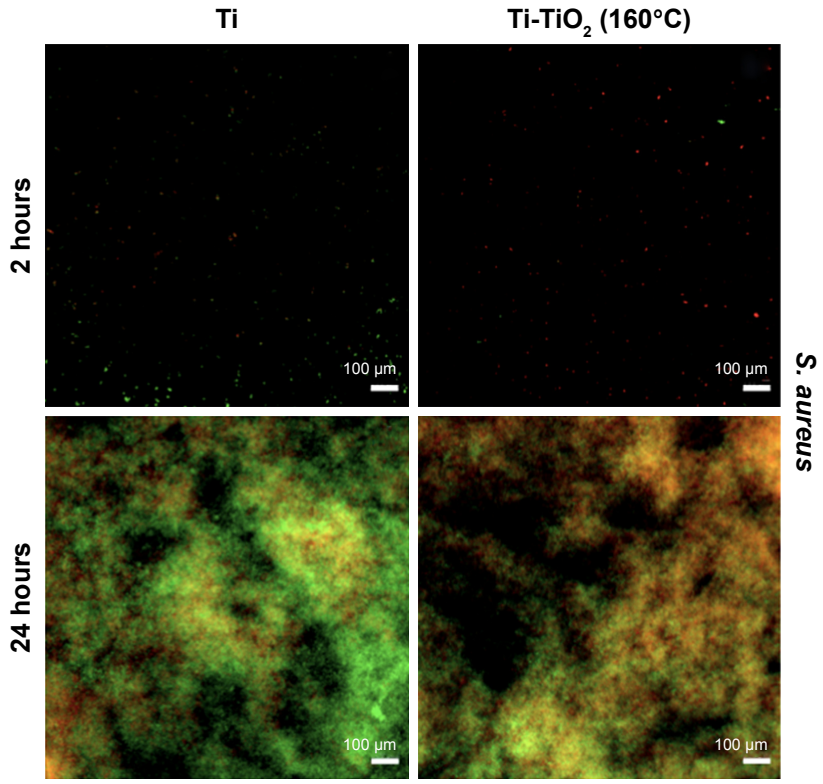

Figure 5 Fluorescent micrographs of *S. aureus* cultured for 2 hours and 24 hours on Ti and Ti-TiO_2 (160°C) samples. SYTO® 9 and propidium iodide were used to stain live (green) and dead (red) bacteria cells, respectively. Scale bars are 100 μm.
Abbreviations: *S. aureus*, *Staphylococcus aureus*; Ti, titanium; TiO_2, titanium dioxide.

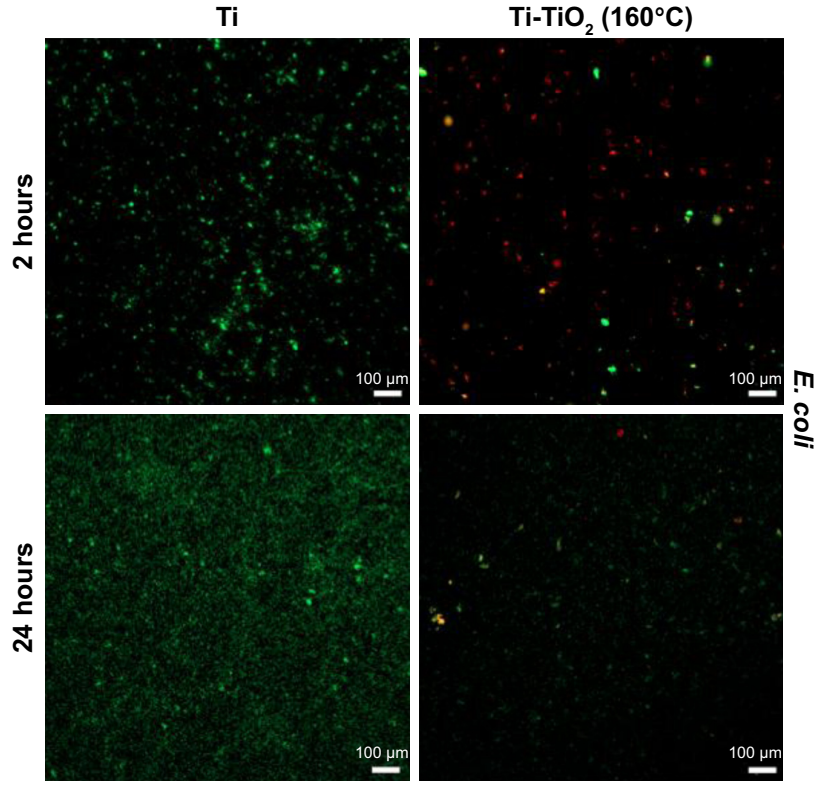

Figure 6 Fluorescent micrographs of *E. coli* cultured for 2 hours and 24 hours on Ti and Ti-TiO_2 (160°C) samples. SYTO® 9 and propidium iodide were used to stain live (green) and dead (red) bacteria cells, respectively. Scale bars are 100 μm.
Abbreviations: *E. coli*, *Escherichia coli*; Ti, titanium; TiO_2, titanium dioxide.

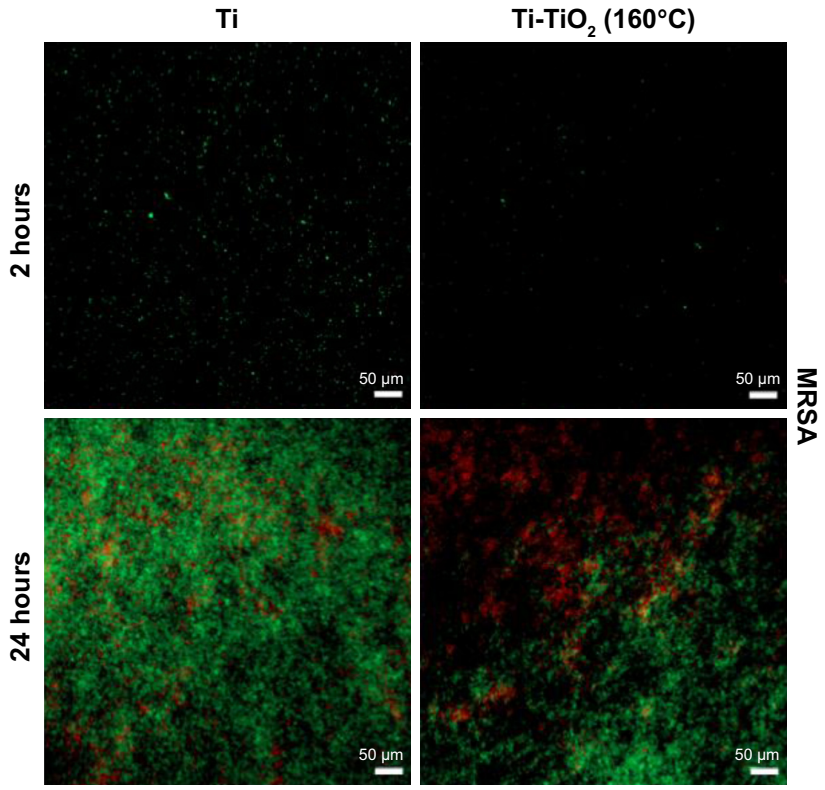

Figure 7 Fluorescent micrographs of MRSA cultured for 2 hours and 24 hours on Ti and Ti-TiO_2 (160°C) samples. SYTO® 9 and propidium iodide were used to stain live (green) and dead (red) bacteria cells, respectively. Scale bars are 50 µm.
Abbreviations: MRSA, methicillin-resistant *Staphylococcus aureus*; Ti, titanium; TiO_2, titanium dioxide.

proteins could interact with bacterial cell membranes and prevent bacterial cells from attaching to the surface.

Cell assays

Since osteoblasts are bone-forming cells, a successful orthopedic implant should promote the initial adhesion and proliferation of osteoblasts on the implant surfaces. However, if the body encapsulates the implant by the formation of a soft fibrous tissue and tries to separate it as much as possible, this is the sign of an unsuccessful implantation. Thus, orthopedic implants should be able to minimize fibrous tissue formation and to maximize new bone generation. In other words, the modified Ti implant in our study should be able to promote osteoblast functions while suppressing fibroblast functions.

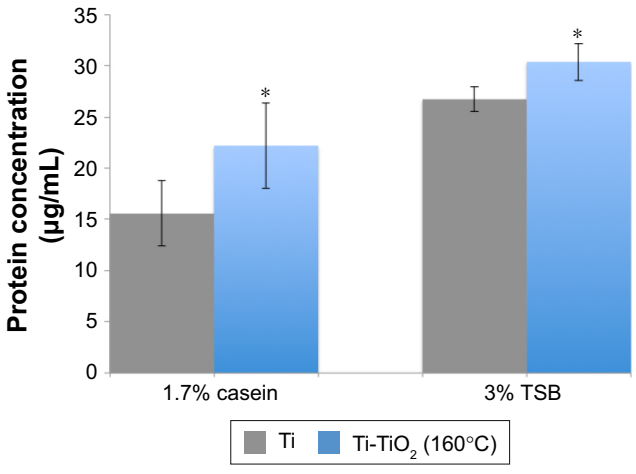

Figure 8 The amount of adsorbed casein protein and total proteins on sample surfaces after 24 hours of culture in a 1.7% casein solution and 3% TSB medium. Data represent mean ± SD, N=3. *$p<0.05$ compared with Ti control (labeled as Ti) in the same tested solution.
Abbreviations: TSB, tryptic soy broth; Ti, titanium; TiO_2, titanium dioxide.

In vitro cell results indicated that initial osteoblast adhesion (after 4 hours of culture) on all Ti-TiO_2 samples was significantly higher than that measured on Ti control samples (Figure 9). In our previous antimicrobial study, Ti-TiO_2 (160°C) samples showed the best antibacterial efficiency toward all types of bacteria; thus, Ti-TiO_2 (160°C) and Ti control substrates were chosen to investigate the effect of the ALD-TiO_2 coatings on osteoblast proliferation. As a result, after 5 days of culture, osteoblast cell numbers on Ti-TiO_2 (160°C) samples were 30% higher than those measured on Ti control samples (Figure 10). This enhanced osteoblast cell adhesion and proliferation can be explained by the increased surface nanoroughness and surface energy of the TiO_2-coated samples, which allows the osteoblasts to adhere in greater numbers due to the higher cell-surface interactions.

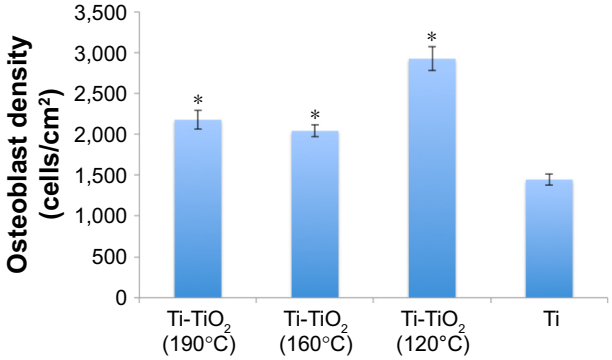

Figure 9 Osteoblast adhesion on Ti samples with different TiO_2 coatings after 4 hours of culture. Data represent mean ± SD, N=3. *$p<0.05$ compared with Ti control (labeled as Ti).
Abbreviations: Ti, titanium; TiO_2, titanium dioxide.

Four-hour and 24-hour experiments were conducted with fibroblasts on Ti control and all TiO_2-coated samples. Results indicated that less fibroblasts adhered on all TiO_2-coated samples compared with Ti control samples (Figure 11). This can be interpreted as follows: TiO_2 coatings selectively promoted osteoblast functions while suppressing undesired fibroblast functions.

Discussion

Implant surfaces play a fundamental role in determining their success due to their control over initial biological events. To develop biomaterials with combined biocompatible and antimicrobial surfaces, various surface modification or coating methods have been investigated.[39–41] In the present study, ALD, a well-established coating technique that is based on the sequential use of self-terminating surface reactions, was used to produce TiO_2 coatings at the nanoscale with different surface morphology and topography on the top of Ti substrates by controlling coating temperatures. Compared to other coating techniques, ALD is more adaptable for growing uniform films on large areas with precise film thickness control. In addition, the surface morphology of the ALD-grown TiO_2 films can be well controlled to achieve favorable nanoroughness and crystallinity.[31,42]

In this study, TiO_2 coatings were deposited onto the Ti substrates by adjusting the reactor temperatures from 120°C and 160°C to 190°C. Morphological observations by SEM (Figure 1A–D) indicated that all TiO_2 coatings were composed of grains with sizes <200 nm and exhibited remarkable nanorough surfaces that were obviously different from Ti controls. It was noted that agglomeration occurred with an increase in temperature and the apparent variability in the TiO_2 coating observed in each SEM image was largely attributable to unevenness of the Ti substrate. RMS roughness values obtained from AFM (Figure 2) confirmed the increased surface nanoroughness on the TiO_2-coated samples quantitatively. XRD analysis was performed to determine the crystalline structure of the TiO_2 thin layers (Figure 3). The XRD patterns of all the Ti-TiO_2 (190°C) exhibited additional peaks at 2θ=25.4° and 48.0° (an indicator of the anatase TiO_2 phase) compared to all other samples, which is in agreement with previous reports indicating the formation of crystalline TiO_2 films at higher temperatures.[43] Surface wettability and associated surface energy affected by surface chemistry and surface topography are of prime importance for the optimization of surrounding biological activities. The values of contact angles for deionized water over Ti samples, as shown in Table 2, indicated slightly higher surface hydrophilicity for the TiO_2-coated samples compared to the Ti controls. These findings are consistent with the many previous studies showing that

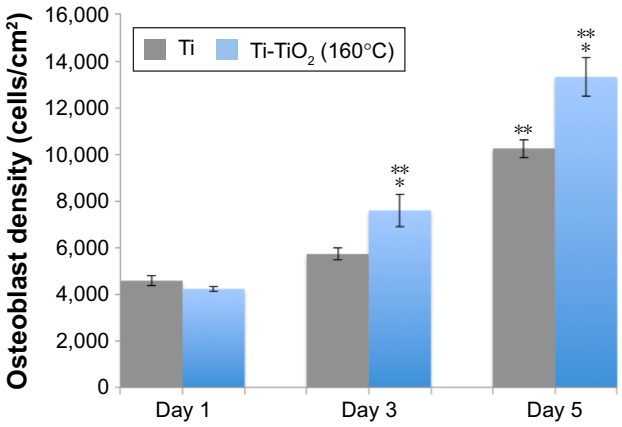

Figure 10 Osteoblast proliferation on Ti and Ti-TiO_2 (160°C) samples. Data represent mean ± SD. N=3. *$p<0.05$ compared with Ti at the same time period, **$p<0.05$ compared with the same sample (Day 1).
Abbreviations: Ti, titanium; TiO_2, titanium dioxide.

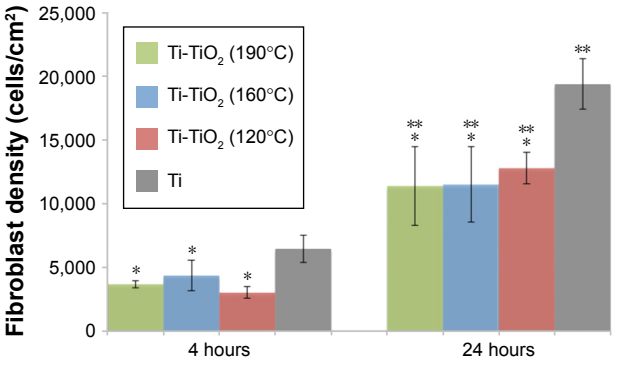

Figure 11 Fibroblast adhesion and growth on Ti and Ti-TiO_2 samples. Data represent mean ± SD. *$p<0.05$ compared with Ti control at the same time period, **$p<0.05$ compared with the same sample (4 hours).
Abbreviations: Ti, titanium; TiO_2, titanium dioxide.

increased surface nanoroughness could contribute to increased wettability and, thus, greater surface energy.[18]

Once the sample surfaces were characterized, we proceeded to evaluate the effect of these TiO_2 coatings on biological activities. Infection has been reported to be a leading cause of the implant failure. Most of the orthopedic implant-related infections are caused by *Staphylococci* (gram-positive bacteria). Among them, *S. aureus* has been identified as the predominant pathogen. In addition, gram-negative bacteria (*E. coli*) also account for a small proportion of these infections.[6] Here, it was found that the TiO_2 coatings were shown to significantly inhibit the adhesion and growth of both *S. aureus* (Figures 4A and 5) and *E. coli* (Figures 4B and 6), and the antibacterial efficiency was achieved all above 80% impressively. It has been reported that this antibacterial effect could be attributed presumably to the semiconductor nature of TiO_2.[44] Upon exposure to UV for 30 minutes in the beginning, the photoactivated TiO_2 coatings could result in the destruction of both gram-positive and gram-negative bacteria. Photoactivated surfaces as reported are capable of killing more gram-negative bacteria than gram-positive bacteria due to the difference in cell wall structure and peptidoglycan thickness, which was concordant with our results.[45]

In addition, since more and more people become infected with bacteria that are resistant to antibiotics, we also tested the antibacterial effect of the TiO_2 coatings against MRSA. Results indicated that Ti-TiO_2 (160°C) samples exhibited a notable decrease in MRSA growth compared with all other TiO_2-coated samples and Ti control as well (Figures 4C and 7). Apart from the photocatalysis action, another possible explanation is that the increased surfaces roughness at the nanoscale could limit the number of anchoring points for these bacteria and further to decrease bacterial adhesion and growth. Herein, although numerous other studies indicated that crystalline structures compared to amorphous structures could further decrease bacterial adhesion and growth, no significant antibacterial result was found for this on Ti-TiO_2 (190°C) samples.[19,20] This might be attributed to the appearance of agglomeration at the beginning of phase transition from an amorphous to a crystalline state.

Although the exact mechanism of how bacteria respond to nano-phase surfaces is not well understood, it is well known that for implanted materials, which are coated with proteins once inserted, it is the adsorbed protein rather than the material surface itself to which cells or bacteria initially respond.[46] Therefore, in this case, the proteins in the bacterial culture medium that adsorbed differently to Ti-TiO_2 (160°C) and Ti control substrates were investigated. Increased protein adsorption (specifically casein protein, which is known to inhibit bacterial growth) was demonstrated on the TiO_2-coated samples. Additionally, this behavior was consistently observed on other materials with nanostructures as reported in previous studies.[47–49] These results together show that surfaces with higher nanoroughness and unique surface energy (~38.79 mJ/m^2) allow more bacteria-repelling proteins with closer surface tension to adsorb to the surface, which could further interact with bacteria cell membranes and prevent bacteria cells from attaching to the surface.

Transitioning focus to the cells, an ideal orthopedic implant should be able to minimize fibrous tissue formation and maximize new bone generation. For this reason, osteoblast and fibroblast adhesion and proliferation were conducted. After 4 hours of culture, more osteoblasts attached to all three series of Ti-TiO_2 samples than Ti controls, suggesting that the TiO_2 coatings can promote the initial adhesion of osteoblasts (Figure 9). Osteoblast proliferation assays were conducted on selected Ti-TiO_2 (160°C) and Ti control substrates for up to 5 days. There was no significant difference for the osteoblast growth on both samples after 1 day of culture. However, after 3 and 5 days of culture, the osteoblast numbers on TiO_2-coated samples were around 30% higher than those measured on the Ti control samples (Figure 10). On the contrary, it was found that after 4 hours and 24 hours of culture, TiO_2-coated samples showed lower fibroblast densities compared to the Ti control samples (Figure 11). Interestingly, osteoblast adhesion on Ti samples was found to be directly proportional to initial surface energy of those samples, while the adhesion of fibroblasts exhibited an inverse trend from that observed for osteoblasts as shown in Figure 12. The outcome of the cell experiments could be explained presumably as the substrates with nanostructures might selectively adsorb more vitronectin to which osteoblasts (being more hydrophilic and smaller than other proteins in serum such as fibronectin) have a high affinity. Although this is a speculation at this point and more studies are needed to verify this, previous studies have reported greater vitronectin adsorption on nano-phase materials with higher surface energy.[17]

What is more, it is interesting to consider why varying nanoscale surface roughness and associated surface energy has such different effects on bacteria versus osteoblasts. Compared to the flexible phospholipid cytoplasmic membrane of mammalian cells, the peptidoglycan bacterial cell walls are more rigid and thus less sensitive to nanosurface structures with relatively high surface energy.[50] Taken together, these results suggest that surface energy is an important criterion in

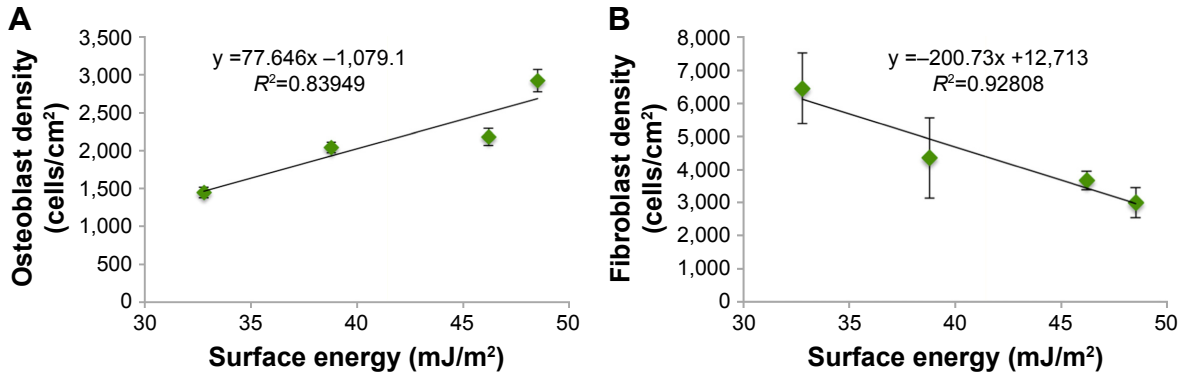

Figure 12 (**A**) Osteoblast and (**B**) fibroblast cell density (after 4 hours of culture) was directly proportional to the surface energy on Ti controls and Ti-TiO_2 samples. Error bars represent SD.
Abbreviations: Ti, titanium; TiO_2, titanium dioxide.

the design of implants to selectively inhibit bacterial adhesion while promoting desirable cell functions.

Conclusion

Nanostructured TiO_2 coatings on Ti-based implants using the ALD technique showed promising antimicrobial efficacy toward gram-positive bacteria (*S. aureus*), gram-negative bacteria (*E. coli*), and antibiotic-resistant bacteria (MRSA). In addition, it was found that the TiO_2 coating stimulated osteoblast adhesion and proliferation while suppressing fibroblast adhesion and proliferation compared to uncoated materials. Mechanistically, data revealed that the increased protein (specifically casein) adsorption, presumably due to the increased surface nanoroughness and surface energy, contributed to these antibacterial properties. Additionally, results suggested that surface energy as another important factor in determining subsequent cell/bacteria responses could be modulated to certain values (~38.79 mJ/m^2) to achieve a variety of desirable biological functions simultaneously. In all, owing to the enhanced biocompatibility and antibacterial activity without using pharmaceutical agents, there is strong potential to apply this ALD-TiO_2 coating in the field of orthopedic implants.

Acknowledgments

The authors would like to thank George J, Kostas Nanoscale Technology and Manufacturing Research Center, Northeastern University, for providing the facilities for material characterization and Run (Kanny) Chang for XRD characterization. Also, the authors would like to acknowledge Ultratech Company (Waltham, MA, USA) for ALD technical support and funding. The abstract of this paper was presented at the Northeastern University Biomaterials Day 2017 as a poster presentation with interim findings. The poster's abstract was published online in "Poster Abstracts" by the Society for Biomaterials.

Disclosure

The authors report no conflicts of interest in this work.

References

1. Elias CN, Lima JHC, Valiev R, Meyers MA. Biomedical applications of titanium and its alloys. *JOM*. 2008;60(3):46–49.
2. Drnovšek N, Rade K, Milačič R, et al. The properties of bioactive TiO_2 coatings on Ti-based implants. *Surf Coat Technol*. 2012;209:177–183.
3. Boos C, Fink K, Stomberg P, et al. The influence of bone quality and the fixation procedure on the primary stability of cementless implanted tibial plateaus. *Biomed Tech*. 2008;53(2):70–76.
4. Darouiche RO. Treatment of infections associated with surgical implants. *N Engl J Med*. 2004;350(14):1422–1429.
5. Song Z, Borgwardt L, Høiby N, Wu H, Sørensen TS, Borgwardt A. Prosthesis infections after orthopedic joint replacement: the possible role of bacterial biofilms. *Orthop Rev (Pavia)*. 2013;5(2):65–71.
6. Raphel J, Holodniy M, Goodman SB, Heilshorn SC. Multifunctional coatings to simultaneously promote osseointegration and prevent infection of orthopaedic implants. *Biomaterials*. 2016;84:301–314.
7. Brennan SA, Ní Fhoghlú C, Devitt BM, O'Mahony FJ, Brabazon D, Walsh A. Silver nanoparticles and their orthopaedic applications. *Bone Joint J*. 2015;97-B(5):582–589.
8. Sambale F, Wagner S, Stahl F, et al. Investigations of the toxic effect of silver nanoparticles on mammalian cell lines. *J Nanomater*. 2015;2015:136765.
9. Goodman SB, Yao Z, Keeney M, Yang F. The future of biologic coatings for orthopaedic implants. *Biomaterials*. 2013;34(13):3174–3183.
10. Lorenzetti M, Dogša I, Stošicki T, et al. The influence of surface modification on bacterial adhesion to titanium-based substrates. *ACS Appl Mater Interfaces*. 2015;7(3):1644–1651.
11. Kargupta R, Bok S, Darr CM, et al. Coatings and surface modifications imparting antimicrobial activity to orthopedic implants. *Wiley Interdiscip Rev Nanomed Nanobiotechnol*. 2014;6(5):475–495.
12. Bagherifard S, Hickey DJ, de Luca AC, et al. The influence of nanostructured features on bacterial adhesion and bone cell functions on severely shot peened 316L stainless steel. *Biomaterials*. 2015;73:185–197.
13. Santiago-Medina P, Sundaram PA, Diffoot-Carlo N. Titanium oxide: a bioactive factor in osteoblast differentiation. *Int J Dent*. 2015;2015:357653.

14. Aboelzahab A, Azad AM, Dolan S, Goel V. Mitigation of *Staphylococcus aureus*-mediated surgical site infections with IR photoactivated TiO_2 coatings on Ti implants. *Adv Health Mater*. 2012;1(3):285–291.
15. Rupp F, Haupt M, Klostermann H, et al. Multifunctional nature of UV-irradiated nanocrystalline anatase thin films for biomedical applications. *Acta Biomater*. 2010;6(12):4566–4577.
16. Visai L, De Nardo L, Punta C, et al. Titanium oxide antibacterial surfaces in biomedical devices. *Int J Artif Organs*. 2011;34(9):929–946.
17. Smith LL, Niziolek PJ, Haberstroh KM, Nauman EA, Webster TJ. Decreased fibroblast and increased osteoblast adhesion on nanostructured NaOH-etched PLGA scaffolds. *Int J Nanomedicine*. 2007;2(3):383–388.
18. Zhao X, Wang G, Zheng H, et al. Delicate refinement of surface nanotopography by adjusting TiO_2 coating chemical composition for enhanced interfacial biocompatibility. *ACS Appl Mater Interfaces*. 2013;5(16):8203–8209.
19. Rani VV, Vinoth-Kumar L, Anitha VC, Manzoor K, Deepthy M, Shantikumar VN. Osteointegration of titanium implant is sensitive to specific nanostructure morphology. *Acta Biomater*. 2012;8(5):1976–1989.
20. Puckett SD, Taylor E, Raimondo T, Webster TJ. The relationship between the nanostructure of titanium surfaces and bacterial attachment. *Biomaterials*. 2010;31(4):706–713.
21. Yao JK, Huang HL, Ma JY, et al. High refractive index TiO_2 film deposited by electron beam. *J Surf Eng*. 2009;25(3):257–260.
22. López-Huerta F, Cervantes B, González O, et al. Biocompatibility and surface properties of TiO_2 thin films deposited by DC magnetron sputtering. *Materials*. 2014;7(6):4105–4117.
23. Yang Y, Park S, Liu Y, et al. Development of sputtered nanoscale titanium oxide coating on osseointegrated implant devices and their biological evaluation. *Vacuum*. 2009;83(3):569–574.
24. Borras A, Sanchez-Valencia JR, Widmer R, Rico VJ, Justo A, Gonzalez-Elipe AR. Growth of crystalline TiO_2 by plasma enhanced chemical vapor deposition. *Cryst Growth Des*. 2009;9(6):2868–2876.
25. Iatsunskyi I, Jancelewicz M, Nowaczyk G, et al. Atomic layer deposition TiO_2 coated porous silicon surface: structural characterization and morphological features. *Thin Solid Films*. 2015;589:303–308.
26. Kim HW, Koh YH, Li LH, Lee S, Kim HE. Hydroxyapatite coating on titanium substrate with titania buffer layer processed by sol-gel method. *Biomaterials*. 2004;25(13):2533–2538.
27. Johnson RW, Hultqvist A, Bent SF. A brief review of atomic layer deposition: from fundamentals to applications. *Mater Today*. 2014;17(5):236–246.
28. Xie Q, Jiang YL, Detavernier C, et al. Atomic layer deposition of TiO_2 from tetrakis-dimethyl-amido titanium or Ti isopropoxide precursors and H_2O. *J Appl Phys*. 2007;102(8):083521.
29. Chaukulkar RP, Agarwal S. Atomic layer deposition of titanium dioxide using titanium tetrachloride and titanium tetraisopropoxide as precursors. *J Vac Sci Technol A*. 2013;31(3):031509.
30. Aarik J, Aidla A, Mändar H, Uustare T. Atomic layer deposition of titanium dioxide from $TiCl_4$ and H_2O: investigation of growth mechanism. *Appl Surf Sci*. 2001;172(1–2):148–158.
31. Miikkulainen V, Leskela M, Ritala M, Puurunen RL. Crystallinity of inorganic films grown by atomic layer deposition: overview and general trends. *J Appl Phys*. 2013;113(2):021301.
32. Aarik J, Aidla A, Uustare T, Sammelselg V. Morphology and structure of TiO_2 thin films grown by atomic layer deposition. *J Cryst Growth*. 1995;148(3):268–275.
33. Jin C, Liu B, Lei Z, Sun J. Structure and photoluminescence of the TiO_2 films grown by atomic layer deposition using tetrakis-dimethylamino titanium and ozone. *Nanoscale Res Lett*. 2015;10:95.
34. Owens DC, Wendt RC. Estimation of the surface free energy of polymers. *J Appl Polym Sci*. 1969;13(8):1741–1747.
35. Gittens RA, Olivares-Navarrete R, Schwartz Z, Boyan BD. Implant osseointegration and the role of microroughness and nanostructures: lessons for spine implants. *Acta Biomater*. 2014;10(8):3363–3371.
36. Miyauchi T, Yamada M, Yamamoto A, et al. The enhanced characteristics of osteoblast adhesion to photofunctionalized nanoscale TiO_2 layers on biomaterials surfaces. *Biomaterials*. 2010;31(14):3827–3839.
37. Silverwood RK, Fairhurst PG, Sjöström T, et al. Analysis of osteoclastogenesis/osteoblastogenesis on nanotopographical titania surfaces. *Adv Healthc Mater*. 2016;5(8):947–955.
38. Liu K, Cao M, Fujishima A, Jiang L. Bio-inspired titanium dioxide materials with special wettability and their applications. *Chem Rev*. 2014;114(19):10044–10094.
39. Wu S, Weng Z, Liu X, Yeung KWK, Chu P. Functionalized TiO_2 based nanomaterials for biomedical applications. *Adv Funct Mater*. 2014;24(35):5464–5481.
40. Hou NY, Perinpanayagam H, Mozumder MS, Zhu J. Novel development of biocompatible coatings for bone implants. *Coatings*. 2015;5(4):737–757.
41. Wang G, Li J, Lv K, et al. Surface thermal oxidation on titanium implants to enhance osteogenic activity and in vivo osseointegration. *Sci Rep*. 2016;6:31769.
42. McDonnell S, Longo RC, Seitz O, et al. Controlling the atomic layer deposition of titanium dioxide on silicon: dependence on surface termination. *J Phys Chem C*. 2013;117(39):20250–20259.
43. Abendroth B, Moebus T, Rentrop S, et al. Atomic layer deposition of TiO_2 from tetrakis(dimethylamino) titanium and H_2O. *Thin Solid Films*. 2013;545:176–182.
44. Kubacka A, Diez MS, Rojo D, et al. Understanding the antimicrobial mechanism of TiO_2-based nanocomposite films in a pathogenic bacterium. *Sci Rep*. 2014;4:4134.
45. Depan D, Misra RD. On the determining role of network structure titania in silicone against bacterial colonization: mechanism and disruption of biofilm. *Mater Sci Eng C Mater Biol Appl*. 2014;34:221–228.
46. Anselme K, Davidson P, Popa AM, Giazzon M, Liley M, Ploux L. The interaction of cells and bacteria with surfaces structured at the nanometre scale. *Acta Biomater*. 2010;6(10):3824–3846.
47. Liu L, Ercan B, Sun L, Ziemer KS, Webster TJ. Understanding the role of polymer surface nanoscale topography on inhibiting bacteria adhesion and growth. *ACS Biomater Sci Eng*. 2016;2(1):122–130.
48. Abadian PN, Goluch ED. Surface plasmon resonance imaging (SPRi) for multiplexed evaluation of bacterial adhesion onto surface coatings. *Anal Methods*. 2015;7:115–122.
49. Nune C, Xu W, Misra RD. The impact of grafted modification of silicone surfaces with quantum-sized materials on protein adsorption and bacterial adhesion. *J Biomed Mater Res A*. 2012;100(12):3197–3204.
50. Gallo J, Holinka M, Moucha CS. Antibacterial surface treatment for orthopaedic implants. *Int J Mol Sci*. 2014;15(8):13849–13880.